Open Archive TOULOUSE Archive Ouverte (OATAO)
OATAO is an open access repository that collects the work of Toulouse researchers and makes it freely available over the web where possible.

This is an author-deposited version published in : http://oatao.univ-toulouse.fr/
Eprints ID : 16032

To link to this article : DOI : 10.1002/celc.201500375
URL : http://dx.doi.org/10.1002/celc.201500375

To cite this version : Pébère, Nadine and Vivier, Vincent *Local Electrochemical Measurements in Bipolar Experiments for Corrosion Studies*. (2016) ChemElectroChem, vol. 3 (n° 3). pp. 415-421. ISSN 2196-0216

Any correspondence concerning this service should be sent to the repository administrator: staff-oatao@listes-diff.inp-toulouse.fr

DOI: 10.1002/celc.201500375

Local Electrochemical Measurements in Bipolar Experiments for Corrosion Studies

Nadine Pébère[a] and Vincent Vivier*[b]

In this work, the local potential and local current were measured with paired Ag/AgCl reference microelectrodes during the corrosion of a 304L stainless-steel (304L SS) sample in bipolar experiments. During a single experiment, it was possible to investigate both the anodic and cathodic domains corresponding to the corrosion of the stainless steel. From these local measurements in non-contact mode, the current/potential curve was obtained, revealing the different reactivities of the 304L SS sample, over a large potential range. The polarisation curve was similar to that usually obtained in a classical three-electrode configuration.

1. Introduction

Corrosion processes and metal dissolution behaviour are usually investigated by using a conventional electrochemical approach, that is, using the metal of interest as the working electrode of a three-electrode system and recording its current and/or potential variations in different conditions. An alternative way to monitor the electrode potential is bipolar electrochemistry, which has already been widely used over recent decades.[1–11] It uses two independent electrodes (i.e. two non-contact electrodes) to apply an electric field in an electrochemical cell that contains a metallic substrate immersed in a conductive medium. It results in a potential distribution along the substrate, allowing the reactivity of the interface to be tuned.

Different aspects of bipolar electrochemistry have recently been reviewed.[1,2] For instance, Fleishman and Oldfield investigated fluidised bed electrodes and described the electrochemical reactions occurring at individual conductive particles.[3,4] Goodridge et al. used arrangements of rods as bipolar electrodes for electro-organic synthesis in a flow cell,[5] whereas Novoa and co-workers used the concept of non-contact measurements to perform electrochemical impedance spectroscopy and to characterise rebar in reinforced concrete.[6,7] Bipolar electrochemistry also allows asymmetric particles to be synthesised by performing electrodeposition in different systems, such as carbon nanotubes and spherical microparticles.[1,8–11] It also allows the motion of small objects to be controlled through the activation of micro- or nanomotors, allowing translational or rotational displacements.[12–16]

Interestingly, the chemical composition of a conducting surface can be tuned by controlling the chemical gradient, using the bipolar electrode for the formation of self-assembled monolayers[17] or for the doping of a polymethylthiophene film.[18] In their seminal work, Duval et al. investigated the influence of an electric field on the electrochemical behaviour of an aluminium surface immersed in nitrate-containing electrolyte.[19]

In recent papers, Björefors and co-workers used bipolar electrochemistry to investigate the corrosion of stainless steels.[20,21] They showed that it is possible to determine the different electrochemical reactions (cathodic reduction, passivity, transpassivity, etc.) that can occur on a single 304L stainless-steel (304L SS) sample immersed in a sulfuric acid solution. In a chloride-containing solution, they demonstrated the pitting corrosion by a pitting gradient (i.e. the number of pits per unit area depending on the distance from the edge of the 304L SS).[21] Interestingly, they also showed that bipolar electrochemistry provides an easy way to simultaneously compare the electrochemical reactivity of different grades of steel by performing post-mortem optical observations of the samples.[20]

In a bipolar system, surface reactivity is usually characterised by using an indirect approach, and different methods have been developed to link the electrochemical reactivity of both anodic and cathodic reactions occurring at the bipolar electrode in order to access to the actual resulting local current. For instance, electrogenerated chemiluminescence (ECL) was shown to quantitatively describe the rates of the electrochemical reactions.[13,22,23] Crooks and co-workers screened for electrocatalysis candidates by using the dissolution of Cr or Ag microbands while varying the composition of the electrocatalysis materials to enhance the oxygen reduction reaction.[24,25]

Direct measurement of the local current remains challenging although amperometric detection has already been reported for capillary electrophoresis (CE) experiments by using two mi-

[a] Dr. N. Pébère
Université de Toulouse
CIRIMAT, UPS/INPT/CNRS, ENSIACET
31030 Toulouse cedex 4 (France)

[b] Dr. V. Vivier
Sorbonne Universités
UPMC Univ Paris 06, CNRS
Laboratoire Interfaces et Systèmes Electrochimiques
4 place Jussieu, F-75005, Paris (France)
E-mail: vincent.vivier@upmc.fr

croband electrodes positioned close to the capillary outlet.[26] By using ferricyanide and ferrocyanide as redox mediators, transient measurement of the current and cyclic voltammograms were recorded as a function of the electric field. This approach was then extended to an array of microband electrodes,[27] and indirect methods such as ECL have already been shown to be efficient for monitoring the reactivity of an array of a thousand bipolar gold electrodes.[23]

The use of local potential sensors for measuring local current in an electrochemical cell was devised some decades ago for pitting corrosion investigations (e.g. determination of the anodic and cathodic areas)[28] and biological applications (e.g. measurement of ionic current),[29] leading to the development of the scanning vibrating electrode technique (SVET)[29,30] and to local electrochemical impedance spectroscopy (LEIS).[31–34] In both cases, the local potential difference between two neighbouring positions was used to evaluate the local current density. In the present work, local electrochemical probes were used to measure potential and current density above a bipolar stainless-steel substrate. The aim of this work is to demonstrate that these local quantities can be estimated by using a simple, cheap system. The accuracy of the measurements will be discussed.

Experimental Section

The experiments were performed in a 6 cm×5 cm×4 cm Teflon cell. The electric field was applied through two carbon-graphite electrodes (5×5 cm^2) located at the two opposite ends, connected to a switching DC power supply 18 V/20 A (Instek, SPS-series), as in the sketch in Figure 1.

A 304L SS plate (5 cm×3 cm×0.1 cm) was used for the investigations. It was embedded in epoxy resin to expose a single face to the electrolyte. The 304L SS electrodes were ground with abrasive paper down to grade P1200, rinsed with deionised water and ethanol, sonicated for 5 min in an EtOH/H_2O mixture and dried in a stream of Ar gas. The SS electrode (bipolar electrode) was then placed at the bottom of the electrochemical cell without further preparation. The corrosive medium was deionised water containing sulfuric acid (0.5 M) and a small concentration of chloride (5 mM). This chloride concentration was chosen to avoid localised corrosion (pitting), but it enables the local potential sensor (Ag/AgCl microelectrode) to behave stably and reproducibly.

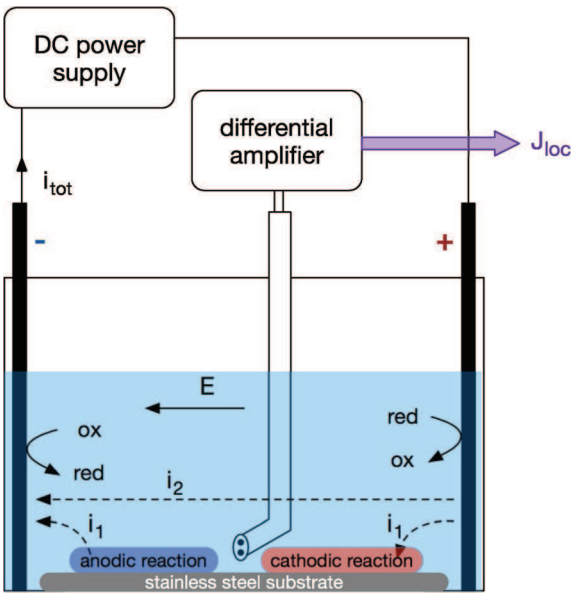

Figure 1. Sketch of the experimental setup used for performing local electrochemical measurements during a bipolar experiment.

Local potential and local current measurements were performed with a paired Ag/AgCl reference microelectrode. It consisted of two silver wires (100 μm in diameter) insulated with cataphoretic paint, except at the tip, and sealed in a theta capillary in epoxy resin. Silver chloride was then deposited on each wire.

The local potential was measured with the micro-reference electrode of the bi-microelectrode, which was the closest to the substrate.

The local current density was determined by measuring the local potential difference $\Delta E_{loc} = E_{ref2} - E_{ref1}$ (where E_{ref1} and E_{ref2} are the local potentials as sensed by the two local Ag/AgCl probes) using Ohm's law for the electrolyte [Eq. (1)]:[32,35,36]

$$j_{loc} = \frac{\Delta E_{loc} \cdot \kappa}{d} \quad (1)$$

where κ is the electrolyte conductivity and d the distance between the two potential probes.

As d is small (about 150 μm), ΔE_{loc} was first amplified with a homemade differential amplifier with variable gain (10–2000). However, as the two probes were slightly different, a small potential difference was noted between them (1–3 mV), which may lead to a significant offset in current after the amplification loop. Therefore, a level shifter had to be used to improve the accuracy of the measurement. From a practical point of view, once the offset had been adjusted, a preliminary experiment was performed in the same electrolyte (i.e. same ionic strength), but containing a redox mediator that reacted at a Pt electrode, and the coefficient κ/d in Equation (1) was experimentally determined from the current measured at the Pt electrode. Note that a similar procedure is commonly used in LEIS experiments.[33,34]

The Ag/AgCl bi-microelectrode was positioned in the vicinity of the substrate by using a stack of three manual linear-translation stages in an *XYZ* configuration (Newport), allowing long displacements with a resolution of about 5 μm. This value is 30 times smaller than the size of the local probe used in the present work. Experiments were also performed with a three-axis positioning system (VP-25XA, Newport) driven by a 100 nm spatial-resolution motion encoder (ESP300, Newport). These two setups not only moved the probe in a parallel plane above the stainless-steel substrate (x, y), but also controlled the distance between the probe and the substrate (z) in the same way as in electrochemical probe techniques already described for corrosion studies.[37,38]

2. Results and Discussion

2.1. Considerations for Local Measurements

It has previously been shown that two different contributions have to be measured in solution for an unambiguous determination of the local current density when the geometry of the electrode is a planar disc, namely the normal and the radial

components.[29,32] With a rectangular electrode, three contributions have to be considered: j_z, the normal component of the local current density perpendicular to the sample surface (which is also perpendicular to the electric field direction); j_x, the x component of the local current density parallel to the sample surface and parallel to the electric field direction; and j_y, the y component of the local current density parallel to the sample surface, but perpendicular to the electric field direction. However, the y component is null, owing to the symmetry of the system. From an experimental point of view, each contribution to the local current density can be measured independently by using a paired microelectrode (see the Experimental Section) placed in the close vicinity of the substrate with the three-axis positioning system.[39]

The maximum electric field used in this work was 10 V (1.67 V cm^{-1}) between the two graphite electrodes, and the distance between the two Ag/AgCl probes forming the bi-microelectrode for measuring the local current density was about 150 μm. Assuming a linear potential drop between the two graphite plates and if the bi-microelectrode used for measuring the local current density is positioned in a plane parallel to the surface of the 304L SS bipolar electrode, a potential difference of 25 mV (corresponding to the product of the electric field and the distance between the two Ag/AgCl reference microelectrodes) is recorded between the two electrodes. This corresponds to the local potential drop probed by the paired microelectrode. However, the potential drop between the two microelectrodes should be 0 mV for a perfectly aligned system perpendicular to the electric field. This can be seen in Figure 2, where the potential and current distributions calculated by using the finite element method (FEM) for an electrochemical cell, with or without a SS bipolar electrode in the bottom. These calculations were performed by using the experimental cell geometry, an electric field of 1.67 V cm^{-1}, and an electrolyte conductivity of 10^{-4} S cm^{-1}. The bipolar electrode was assumed to be a planar conducting boundary (10^5 S cm^{-1}) without any electrochemical reactivity, so the current and potential distributions were simulated independently from the electrochemical processes that may take place at the bipolar electrode interface. From these simulations, it is clear that, in the absence of the SS bipolar electrode (Figure 2a), the only contribution for the local current density is along the x axis (that is, perpendicular to the two electrodes used for applying the electric field), whereas when a conductor is inserted in the electric field (Figure 2b), the z component is no longer negligible. This can be seen by the curvature of the current lines (white lines in Figure 2b). Here, the current through the solution consisted of the sum of the two contributions j_x and j_z. In addition, it is possible to calculate the ratio between the two local current density contributions, as illustrated in Figure 3. In Figure 3a, it is shown that the j_z component is larger than j_x almost everywhere above the conducting substrate, except at the centre ($x=3$ cm) and at the two edges (located at $x=0.5$ and 5.5 cm). At the electrode centre, j_z tends towards 0 because of the symmetry of the system and the boundary conditions used for performing the FEM simulations (distributed resistance on the bipolar electrode, corresponding to a uniform reactivity of the interface). At the edges, the j_z component is smaller than j_x by 2 or 3 orders of magnitude (Figure 3b).

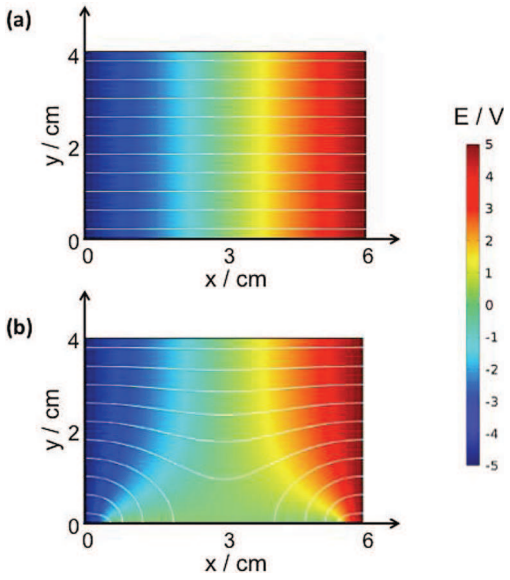

Figure 2. FEM simulations of potential (coloured scale) and current (white line) in the absence (a) and presence (b) of a conductive substrate (5 cm long, positioned at $y=0$ cm in the bottom of the cell). Simulations were performed with the geometry of the cell used for the experiments.

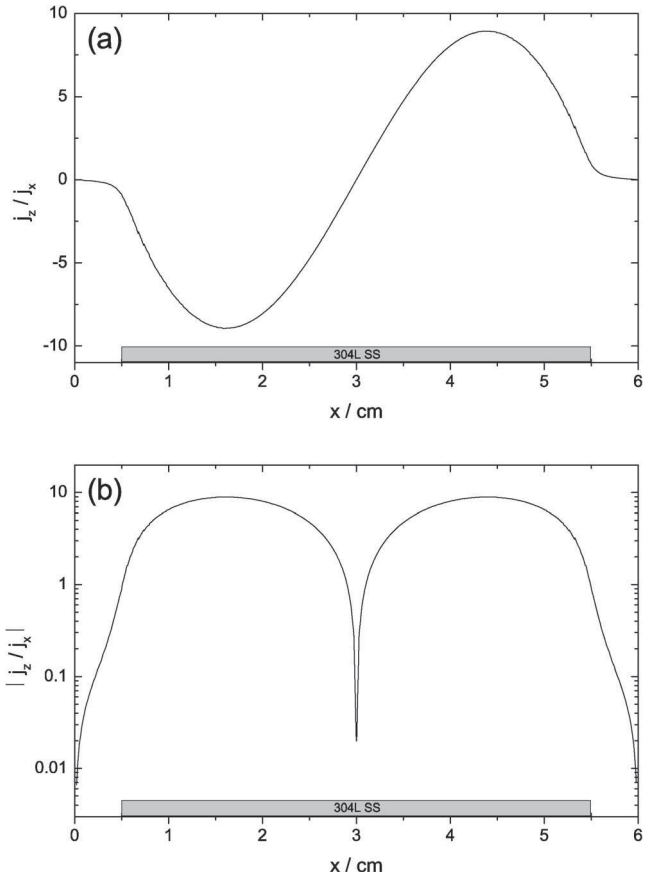

Figure 3. Ratio of the local current densities j_z/j_x (a) and absolute value of this ratio in a semi-log representation (b) calculated at 100 μm from the conducting sample for the FEM simulation presented in Figure 2b.

Figure 3 also shows that measuring the j_z component allows the anodic ($j_z > 0$) and cathodic areas ($j_z < 0$) to be clearly distinguished. The absolute value of the j_z/j_x ratio plotted in a logarithmic representation also shows that j_x is larger at the bipolar electrode centre and at the edges (Figure 3b). Moreover, the j_x component also contains a contribution, owing to the electric field used for polarising the bipolar electrode, which can represent a potential difference of 25 mV for the probe used (as previously discussed), making this contribution difficult to measure, because any tiny variation in the potential corresponding to a local reactivity of the SS bipolar electrode may be lost within this 25 mV. Thus, in the following, we mainly focus on the measurement of the normal component of the local current density, j_z.

2.2. Local Potential above the Bipolar Electrode

In a first step, the local potential was monitored with an Ag/AgCl microprobe [similar to the scanning reference electrode technique (SRET) experiment].[40] The Ag/AgCl microprobe was placed 100 and 300 μm above the 304L SS bipolar electrode (Figure 4) and its potential was measured with respect to a commercial Ag/AgCl electrode by using a differential amplifier to zero the current between these two electrodes.[40,41]

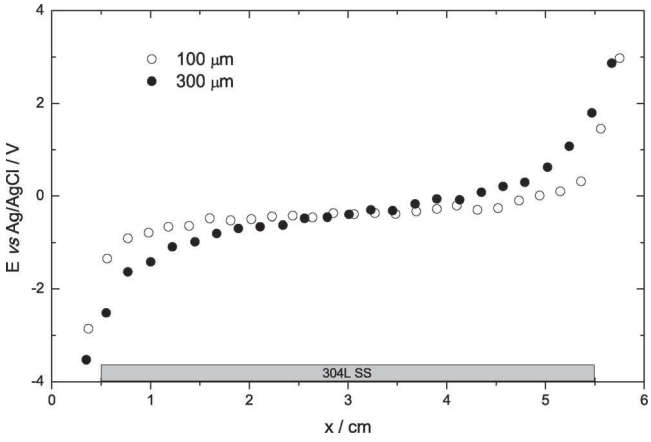

Figure 4. Local potential versus probe position measured at 100 μm (open circles) and 300 μm (black circles) above the 304L SS bipolar electrode in a 0.5 M H_2SO_4 + 5 mM NaCl solution after 2 h polarisation at $\Delta E_{loc} = 10$ V.

When the probe was close to the bipolar electrode (100 μm—open circle in Figure 4), the potential along the sample varied from about −2 to +2 V/Ag/AgCl, indicating that it is possible to simultaneously investigate the anodic and cathodic reactions, as previously shown by Björefors and co-workers.[20,21] In addition, optical observations of the sample after 2 h polarisation clearly showed the transpassive domain with significant dissolution of the material, that is, the passive domain, corresponding to a rather unaffected surface area and the cathodic side on which bubble evolution was observed during the experiment. When the same experiment was carried out by positioning the probe at a greater distance from the substrate, the local potentials were larger, which is in good agreement with the results of the FEM calculation shown in Figure 2. Indeed, the larger the distance between the bipolar SS electrode and the microprobe, the lower the influence of the bipolar SS electrode on the potential distribution.

2.3. Local Current Density above the Bipolar SS Electrode

Figure 5 shows the local current density (j_z component) measured with the paired reference microelectrodes versus their position above the 304L SS bipolar electrode. The potential difference was converted into a local current density by using the procedure described in the Experimental Section (i.e. by using the conversion factor determined experimentally, which depends on both the twin electrode geometry and the electrolyte composition) and assuming that the electrolyte conductivity remains unchanged during the duration of the measurement (2 h). However, it was already shown that bipolar experiments may result in significant ion distribution around a bipolar electrode,[42,43] which may introduce uncertainty in the measurement. Figure 5a clearly reveals the anodic and cathodic domains. The large current densities measured at both edges of the bipolar electrode were ascribed to the cathodic reaction, namely the hydrogen evolution reaction, in agreement with

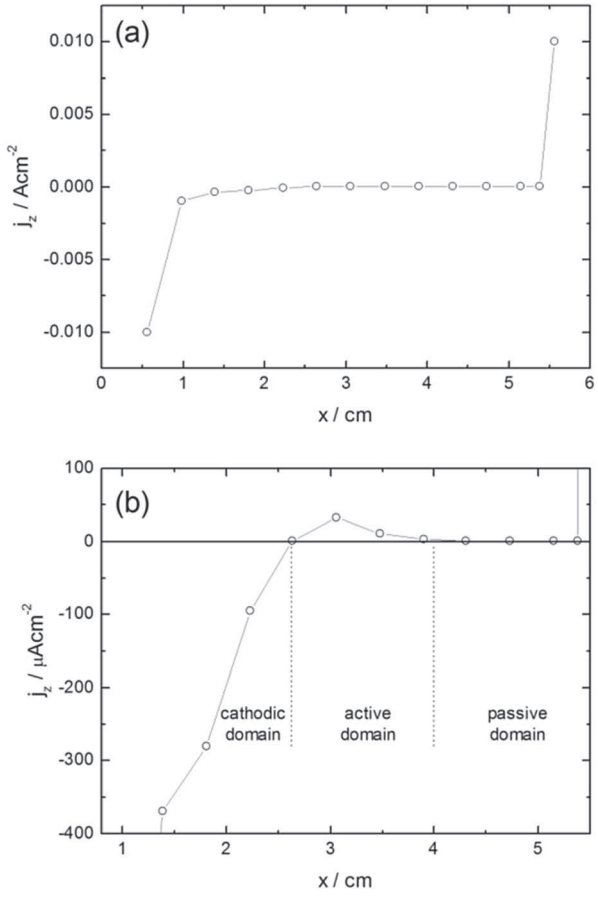

Figure 5. a) Local current versus probe position measured at 100 μm above the 304L SS bipolar electrode in a 0.5 M H_2SO_4 + 5 mM NaCl solution after 2 h polarisation at $\Delta E_{loc} = 10$ V; b) expansion of the small current variations domain. Line is only to provide a visual reference.

the formation of bubbles observed during the experiment, whereas the anodic current was ascribed to the transpassive dissolution of the sample coupled with oxygen evolution. An expansion of the domain corresponding to low current densities (i.e. for a probe position between $x=1$ and 5 cm) clearly shows the transition between the cathodic and the anodic domain at about 2.6 cm (Figure 5b). Moreover, a small current peak, attributed to the activity domain, and then a decrease in the current density, ascribed to the passive domain behaviour of the SS electrode, can be seen in Figure 5b. Thus, the local current density measurements performed above the 304L SS bipolar electrode revealed the different activity domains on a single sample. Similar domains were also reported by Bjorefors and co-workers for a bipolar experiment,[21] but, to the best of our knowledge, this is the first time that local electrochemical measurements were performed to characterise the different reactivities on a steel electrode surface.

When the probe used for monitoring the local current was positioned at about 300 μm from the 304L SS bipolar electrode (data not shown), the signal was much noisier than the results obtained at 100 μm, especially for the passive domain (i.e. for the lower current densities). This is attributed to the fact that the potential difference between the pair of reference microelectrodes becomes smaller as the probe is withdrawn from the substrate and, thus, the signal-to-noise ratio becomes too small to perform an accurate measurement, even after filtering and amplifying the potential difference.

When the probes used for monitoring both the local potential and the local current density where positioned close to the two edges of the bipolar electrode (i.e. between $x=0$ and 0.5 cm, and between $x=5.0$ and 5.5 cm), the measurements are subject to considerable uncertainty, owing to the formation of bubbles, which alter the local potential distribution in these areas. Moreover, forced convection through bubble evolution is not taken into account for the current calculation.

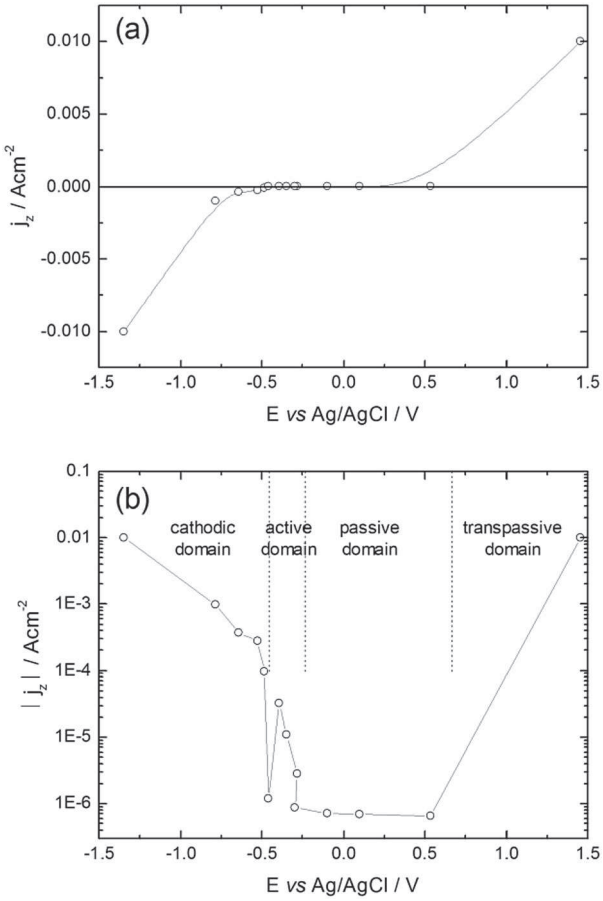

Figure 6. Current/potential curve on the 304L SS bipolar electrode in 0.5 M H_2SO_4 + 5 mM NaCl obtained from the data in Figures 4 and 5: a) linear scale and b) semi-logarithmic scale.

2.4. Current/Potential Curve Obtained from the Local Measurements

From the data presented in Figure 4 (local potential as a function of the probe position) and in Figure 5 (local current as a function of the probe position), it is possible to obtain the current/potential curve on the 304L SS bipolar electrode, as shown in Figure 6a. In Figure 6b, the semi-logarithmic representation of the data clearly shows the different reactivity domains of the SS steel as a function of the potential, and it can be noted that this curve is in good agreement with results presented in the literature and obtained by performing direct measurement on a biased 304L SS electrode. Interestingly, the local measurements enable the anodic and the cathodic domains to be distinguished. Moreover, the variations in the local density reflect the kinetics of the corrosion processes, as for usual electrochemical techniques. From a quantitative point of view, results in this work were obtained by measuring the normal component of the current density, only. As pointed out in the previous discussion, these results led to an underestimation of the overall current density, which is smaller at the centre of the bipolar electrode (corresponding to the small overpotential cathodic domain, the active domain and the passive domain) and larger at the edges (hydrogen evolution reaction and transpassive domain). However, the values obtained in the active domain (in the range of 10 μA cm^{-2}) and in the passive domain (1 μA cm^{-2}) are of the same order of magnitude as those obtained with a steady-state polarisation curve. These preliminary results show that interfacial kinetics may be explored with local measurement above the bipolar electrodes, similarly to that usually performed with electrochemistry, but taking advantage of working on a single sample. For instance, by modulating the amplitude of the applied potential or potential steps, the method will offer a unique way for performing local impedance spectroscopy, or local chronoamperometric studies.

2.5. Local Reactivity along the *y* Direction of the Bipolar Electrode

Table 1 shows the local reactivity along the *y* direction (corresponding to the width of a bipolar electrode) above different domains. Irrespective of the area investigated, it can be seen in Table 1 that the surface reactivity is independent of the *y*-axis position. For instance, above the cathodic domain ($x=$

Table 1. Local potential and local current densities measured at 100 μm along the *y* direction above the 304L SS bipolar electrode in 0.5 M H_2SO_4 + 5 mM NaCl solution after 80 min polarisation at $\Delta E_{loc} = 10$ V.

x [cm]	*y* [cm]	*E* [V vs. Ag/AgCl]	*I* [A]
	1	−0.480	-9.70×10^{-5}
2.2	2	−0.480	-9.50×10^{-5}
	3	−0.482	-9.60×10^{-5}
	1	−0.391	3.40×10^{-5}
3.1	2	−0.393	3.10×10^{-5}
	3	−0.394	3.40×10^{-5}
	1	−0.282	2.60×10^{-6}
4	2	−0.280	2.30×10^{-6}
	3	−0.279	2.70×10^{-6}

2.2 cm), the mean potential was -0.481 ± 0.001 V versus Ag/AgCl for three successive measurements performed on three different locations above the sample ($y = 1$, 2 and 3 cm; $y = 2$, being the centre of the bipolar electrode along the *y* axis), whereas the mean current density was -96 ± 1 μA cm^{-2}. Measurements were not performed on the edge of the bipolar electrode in order to avoid the edge effect on the local potential and current distributions.

2.6. Variation of the Local Reactivity with Time

The local current density measured at the centre of the bipolar electrode is plotted against time in Figure 7. Interestingly, during the first minutes of the experiment, the current density is negative, indicating cathodic behaviour on this part of the surface. The current increases slightly, peaks after about 10 min and then decreases, but still remains positive. The measured local current shows that this part of the surface is firstly cathodic; it then behaves as an active domain before the current density decreases to reach a value considered typical of a passive domain.

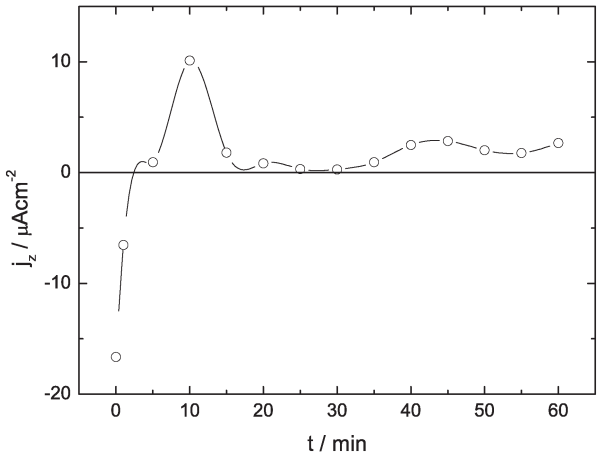

Figure 7. Local current density measured at 100 μm at the centre above the 304L SS bipolar electrode along the width in a 0.5 M H_2SO_4 + 5 mM NaCl solution versus time with polarisation at $\Delta E_{loc} = 10$ V.

The net current flowing through the bipolar electrode is zero, which can be expressed as Equation (2):

$$i_{ox} = -i_{red} \quad (2)$$

For simplicity, let us assume that the cathodic reaction involves a single reaction, whereas the total anodic process is the sum of different contributions (dissolution, passivation, transpassivation). Then, Equation (2) can be rewritten as [Equation (3)]:

$$i_{diss} + i_{pass} + i_{trans} = -i_{red} \quad (3)$$

The introduction of the current density leads to Equation (4):

$$j_{diss} \cdot A_{diss} + j_{pass} \cdot A_{pass} + j_{trans} \cdot A_{trans} = -j_{red} \cdot A_{red} \quad (4)$$

Any variation in $j_{pass} \cdot A_{pass}$ must be compensated by a change of at least one of the other contributions. This shows that the change in the local current density measured as a function of time corresponds to a change in the different surface area. Thus, the boundary, observed after 2 h, between the anodic and cathodic domains (Figures 4, 5 and 6), became shifted along the SS surface with increasing immersion time. The observed variations of reactivity with immersion time were linked to the corrosion behaviour of the 304L SS used in the present study and, of course, they may change depending on the substrate. Moreover, the magnitude of the electric field used for polarising the bipolar electrode is also an important parameter, which controls the potential distribution and, thus, the kinetics of the different reactions occurring on the bipolar electrode surface. In this work, the magnitude of 10 V was selected to show the different anodic domains of the steel, which should not have been possible with a smaller magnitude.

Finally, it should be emphasised that the spatial resolution of the technique is governed by the size of the paired reference microelectrodes used for measuring the local current density as well as the inter-electrode distance. A small inter-electrode distance will result in a small potential difference to be measured. The spatial resolution of the experiments described in this work was of few tens micrometres, allowing the potential difference to be easily amplified and, thus, the DC component of the local current density to be accessed with a low signal to noise ratio. To improve the spatial resolution of the technique, the decrease in the probe size, and thus, the decrease in the distance between the two probes is mandatory, and the use of synchronous detection, similarly to the SVET or the LEIS techniques,[32] is a promising method.

3. Conclusions

In this work, during a bipolar experiment with a stainless-steel electrode, both the local potential and the local current density were measured by using a pair of reference microelectrodes. A preliminary analysis with the help of FEM simulations of the current and potential distributions in the electrochemical cell

showed that both *x* and *z* components of the local current density have to be considered. From the measurement of the *z* component, the different domains corresponding to 304L SS corrosion were determined from the local current densities measured during a single experiment. The local current density was seen to vary as a function of time, indicating a variation of the active surface area of each domain. Interestingly, it can be noted that the current/potential curve is obtainable from the local measurements, showing the usual behaviour of 304L SS polarised with a potentiostat in a three-electrode configuration.

These results demonstrate that local electrochemical measurements (potential or current) can be performed above a bipolar electrode with a spatial resolution in the range of a few tens of micrometres.

Keywords: bipolar corrosion · local electrochemistry · potential distribution · reactivity · stainless steel

[1] G. Loget, D. Zigah, L. Bouffier, N. Sojic, A. Kuhn, *Acc. Chem. Res.* **2013**, *46*, 2513 – 2523.
[2] S. E. Fosdick, K. N. Knust, K. Scida, R. M. Crooks, *Angew. Chem. Int. Ed.* **2013**, *52*, 10438 – 10456; *Angew. Chem.* **2013**, *125*, 10632 – 10651.
[3] M. Fleischmann, J. W. Oldfield, *J. Electroanal. Chem.* **1971**, *29*, 211 – 230.
[4] M. Fleischmann, J. W. Oldfield, *J. Electroanal. Chem.* **1971**, *29*, 231 – 240.
[5] F. Goodridge, C. J. H. King, A. R. Wright, *Electrochim. Acta* **1977**, *22*, 347 – 352.
[6] M. Keddam, X. R. Novoa, V. Vivier, *Corros. Sci.* **2009**, *51*, 1795 – 1801.
[7] M. Keddam, X. R. Novoa, B. Puga, V. Vivier, *Eur. J. Environ. Civil Eng.* **2011**, *15*, 1097 – 1103.
[8] G. Loget, V. Lapeyre, P. Garrigue, C. Warakulwit, J. Limtrakul, M.-H. Delville, A. Kuhn, *Chem. Mater.* **2011**, *23*, 2595 – 2599.
[9] G. Loget, J. Roche, A. Kuhn, *Adv. Mater.* **2012**, *24*, 5111 – 5116.
[10] C. Warakulwit, T. Nguyen, J. Majimel, M.-H. Delville, V. Lapeyre, P. Garrigue, V. Ravaine, J. Limtrakul, A. Kuhn, *Nano Lett.* **2008**, *8*, 500 – 504.
[11] J. C. Bradley, S. Dengra, G. A. Gonzalez, G. Marshall, F. V. Molina, *J. Electroanal. Chem.* **1999**, *478*, 128 – 139.
[12] M. Sentic, G. Loget, D. Manojlovic, A. Kuhn, N. Sojic, *Angew. Chem. Int. Ed.* **2012**, *51*, 11284 – 11288; *Angew. Chem.* **2012**, *124*, 11446 – 11450.
[13] M. Sentic, S. Arbault, B. Goudeau, D. Manojlovic, A. Kuhn, L. Bouffier, N. Sojic, *Chem. Commun.* **2014**, *50*, 10202 – 10205.
[14] W. Duan, W. Wang, S. Das, V. Yadav, T. E. Mallouk, A. Sen, *Annu. Rev. Anal. Chem.* **2015**, *8*, 311 – 333.
[15] T. E. Mallouk, A. Sen, *Sci. Am.* **2009**, *300*, 72 – 77.
[16] Y. Wang, R. M. Hernandez, D. J. Bartlett, Jr., J. M. Bingham, T. R. Kline, A. Sen, T. E. Mallouk, *Langmuir* **2006**, *22*, 10451 – 10456.
[17] C. Ulrich, O. Andersson, L. Nyholm, F. Bjorefors, *Angew. Chem. Int. Ed.* **2008**, *47*, 3034 – 3036; *Angew. Chem.* **2008**, *120*, 3076 – 3078.
[18] S. Inagi, Y. Ishiguro, M. Atobe, T. Fuchigami, *Angew. Chem. Int. Ed.* **2010**, *49*, 10136 – 10139; *Angew. Chem.* **2010**, *122*, 10334 – 10337.
[19] J. Duval, J. M. Kleijn, H. P. van Leeuwen, *J. Electroanal. Chem.* **2001**, *505*, 1 – 11.
[20] S. Munktell, L. Nyholm, F. Björefors, *J. Electroanal. Chem.* **2015**, *747*, 77 – 82.
[21] S. Munktell, M. Tydén, J. Högström, L. Nyholm, F. Björefors, *Electrochem. Commun.* **2013**, *34*, 274 – 277.
[22] R. Liu, C. Zhang, M. Liu, *Sens. Actuators B* **2015**, *216*, 255 – 262.
[23] K.-F. Chow, F. Mavre, J. A. Crooks, B.-Y. Chang, R. M. Crooks, *J. Am. Chem. Soc.* **2009**, *131*, 8364 – 8365.
[24] S. E. Fosdick, R. M. Crooks, *J. Am. Chem. Soc.* **2012**, *134*, 863 – 866.
[25] S. E. Fosdick, S. P. Berglund, C. B. Mullins, R. M. Crooks, *Anal. Chem.* **2013**, *85*, 2493 – 2499.
[26] O. Klett, L. Nyholm, *Anal. Chem.* **2003**, *75*, 1245 – 1250.
[27] O. Ordeig, N. Godino, J. del Campo, F. X. Muñoz, F. Nikolajeff, L. Nyholm, *Anal. Chem.* **2008**, *80*, 3622 – 3632.
[28] I. L. Rosenfeld, I. S. Danilov, *Corros. Sci.* **1967**, *7*, 129 – 142.
[29] L. F. Jaffe, R. Nuccitelli, *J. Cell. Biol.* **1974**, *63*, 614 – 628.
[30] H. S. Isaacs, *J. Electrochem. Soc.* **1991**, *138*, 722 – 728.
[31] R. S. Lillard, P. J. Moran, H. S. Isaacs, *J. Electrochem. Soc.* **1992**, *139*, 1007 – 1012.
[32] V. M.-W. Huang, S.-L. Wu, M. E. Orazem, N. Pebere, B. Tribollet, V. Vivier, *Electrochim. Acta* **2011**, *56*, 8048 – 8057.
[33] G. Baril, C. Blanc, M. Keddam, N. Pebere, *J. Electrochem. Soc.* **2003**, *150*, B488 – B493.
[34] J. B. Jorcin, E. Aragon, C. Merlatti, N. Pebere, *Corros. Sci.* **2006**, *48*, 1779 – 1790.
[35] H. S. Isaacs, *Corros. Sci.* **1988**, *28*, 547 – 558.
[36] G. Galicia, N. Pebere, B. Tribollet, V. Vivier, *Corros. Sci.* **2009**, *51*, 1789 – 1794.
[37] M. B. Jensen, D. E. Tallman, *Electroanal. Chem.* **2011**, *24*, 171 – 286.
[38] C. Gabrielli, E. Ostermann, H. Perrot, V. Vivier, L. Beitone, C. Mace, *Electrochem. Commun.* **2005**, *7*, 962 – 968.
[39] I. Frateur, V. M.-W. Huang, M. E. Orazem, N. Pebere, B. Tribollet, V. Vivier, *Electrochim. Acta* **2008**, *53*, 7386 – 7395.
[40] "Scanning Electrode Techniques for investigating near-surface solution current densities in": R. S. Lillard, *Analytical Methods for Corrosion Science and Engineering* (Eds.: P. Marcus, F. Mansfeld), CRC/Taylor & Francis, Boca Raton, FL, **2005**, pp. 571 – 604.
[41] R. S. Thornhill, U. R. Evans, *J. Chem. Soc.* **1938**, 2109 – 2114.
[42] K. N. Knust, E. Sheridan, R. K. Anand, R. M. Crooks, *Lab Chip* **2012**, *12*, 4107 – 4114.
[43] K. N. Knust, D. Hlushkou, U. Tallarek, R. M. Crooks, *ChemElectroChem* **2014**, *1*, 850 – 857.